tvst

Lens

System for Objective Assessment of the Accommodation Response During Subjective Refraction

Carlos E. García-Guerra[1], Joan A. Martínez-Roda[1], Juan C. Ondategui-Parra[1], Aina Turull-Mallofré[1], Mikel Aldaba[1], and Meritxell Vilaseca[1]

[1] Centre for Sensors, Instruments and Systems Development (CD6), Universitat Politècnica de Catalunya, Terrassa, Spain

Correspondence: Aina Turull-Mallofré, Centre for Sensors, Instruments and Systems Development (CD6), Universitat Politècnica de Catalunya, Rambla Sant Nebridi 10, 08222 Terrassa, Spain.
e-mail: aina.turull@upc.edu

Received: October 13, 2022
Accepted: April 27, 2023
Published: May 23, 2023

Keywords: subjective refraction; accommodation; wavefront refraction

Citation: García-Guerra CE, Martínez-Roda JA, Ondategui-Parra JC, Turull-Mallofré A, Aldaba M, Vilaseca M. System for objective assessment of the accommodation response during subjective refraction. Transl Vis Sci Technol. 2023;12(5):22, https://doi.org/10.1167/tvst.12.5.22

Purpose: To evaluate a system based on a Hartmann–Shack wavefront sensor attached to a phoropter that allows the user to obtain real-time information about the refractive state of the eye and the accommodation response (AR).

Methods: The objective refractions (M_E) and ARs of 73 subjects (50 women, 23 men; ages, 19–69 years) were assessed with the system developed while placing in the phoropter the subjective refraction (M_S) plus a set of trial lenses with differences in spherical equivalent power (ΔM) between ± 2 diopters (D).

Results: The objective estimations (M_E) showed a good correlation with the subjective values (M_S) ($r = 0.989$; $P < 0.001$). The means of the ARs presented a region where the accommodation remained stable (ΔM from $+2$ D to about 0 D), followed by another in which the response increased progressively (ΔM from about 0 to -2 D) with the magnitude of the accommodation stimulus. The analysis of variance within subjects applied to ARs introducing age and M_S as covariates showed an increasing effect size of age from medium to large between ΔM of -0.5 and -2 D. In contrast, M_S had a medium effect size (between ΔM of $+2$ and 0 D).

Conclusions: The implemented system permitted an objective estimation of the refraction of the eye and its AR. Because it is coupled to a phoropter, the system can be used to retrieve the AR during subjective refraction procedures.

Translational Relevance: The developed system can be used as a supporting tool during subjective refraction to provide certainty about the true state of accommodation.

Introduction

Subjective refraction is currently the gold standard procedure for assessing refractive errors in clinical practice. This process consists of determining the combination of lenses that allows the patient to resolve the smallest optotype in the absence of accommodation.[1,2] Therefore, correct control of accommodation, which ensures that it is not activated (i.e., the ciliary muscle remains relaxed), is crucial for the success of the test, especially in children and young adults, who have the greatest accommodation capacity and an involuntary tendency to accommodate.[3,4]

Different techniques can be used to control accommodation during subjective refraction. The most effective method is the use of cycloplegic drops to temporarily paralyze the ciliary muscle,[5,6] the organ in charge of activating accommodation. However, its effects may persist beyond the test by limiting visual capacity, which may be uncomfortable for the patient. Another method that is used is the fogging technique,[1,7] which involves placing trial lenses with positive spherical power in front of the eye so that accommodation is relaxed by artificially making the eye more myopic. Even though fogging has been proven effective in most cases,[8] the success of its implementation depends to some extent on the expertise of the clinician,

particularly in children, and there is no evidence about the true state of accommodation.

Accommodation can be studied indirectly in an objective manner from estimations of the spherical refractive state of the eye.[9] Using this principle, different aspects related to the accommodation have been investigated, especially under laboratory conditions.[10–15] Hartmann–Shack (HS) wavefront sensors[16] have proven reliable for analysis of the accommodation response (AR),[9,17] and they have permitted a better understanding of the relation between aberrations and accommodation. For example, not only variations with accommodation of higher order aberrations (HOAs)[9] but also their impact on the accommodative response[18] have been shown. In fact, the larger accommodation errors for near targets (lags) in myopes have been associated with a larger amount of HOA observed in this population.[19,20] In some works, the AR has been improved by using multifocal patterns,[18,21] which could aid improvement of multifocal lens designs.[21] A variety of commercially available stand-alone tabletop[22–24] and handheld[25,26] instruments can provide objective estimations of the refractive error. In addition, systems that integrate HS wavefront sensors with digital phoropters have been developed.[23] In the standard subjective refraction procedure in clinical practice, these kinds of instruments are mainly used to obtain a starting point,[27] not for determining a final prescription, due to a lack of control of accommodation.[28] Thus, the objective refraction result is then refined using subjective refraction, first by adding positive or fogging lenses to control accommodation and then reducing its power until maximum plus power for best visual acuity is achieved.[2] Beyond the starting refraction, real-time availability of the refractive state of the eye could be of interest for clinicians to be certain about the true AR during the subjective test, especially when the fogging technique is used.

In this study, we present an open-field instrument that provides monocular estimations of the refractive state of the eye every 100 ms. The system was coupled to a conventional phoropter to retrieve the AR in conditions similar to those expected during clinical subjective refraction based on a set of measurements while performing a sweep through several spherical trial lenses. For validation purposes, the responses obtained with the system are compared to expected behaviors for specific ranges of age and refractive errors. The developed system may be used to monitor the AR during subjective procedures and may help clinicians to validate its behavior at any time, ensuring that it remains relaxed and that corrective actions can be taken if needed, especially when using the fogging technique to control accommodation.

Methods

Experimental System

The optical design and a photograph of the instrument are shown in Figure 1. The system, which works coupled to a phoropter, operates as follows: Collimated

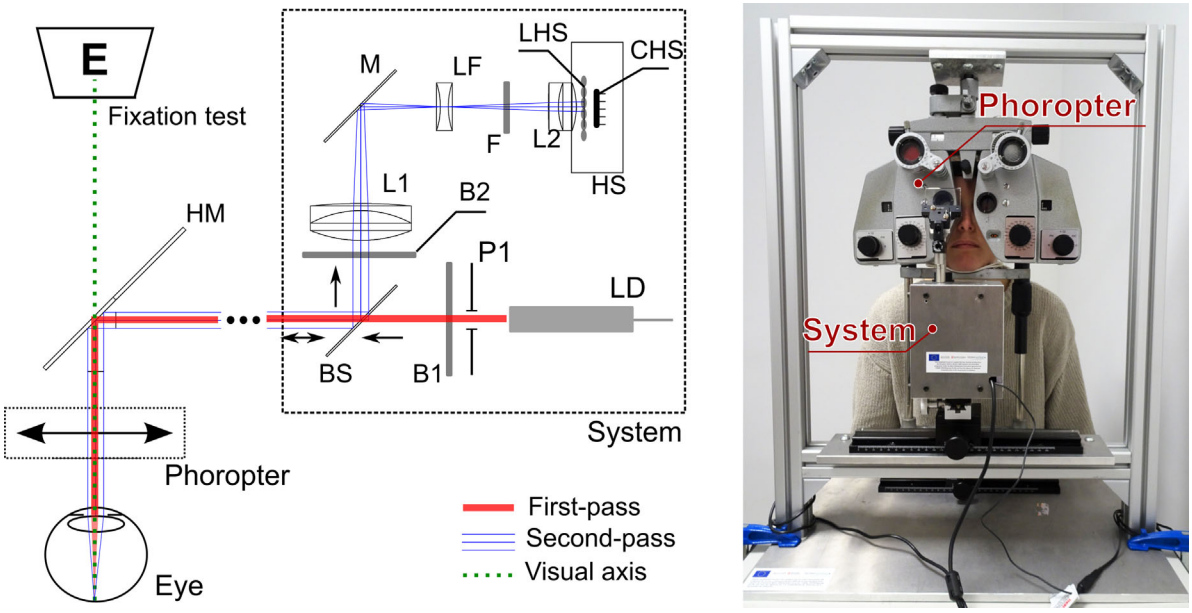

Figure 1. Optical design (*left*) and photograph of system developed while coupled to the phoropter (*right*).

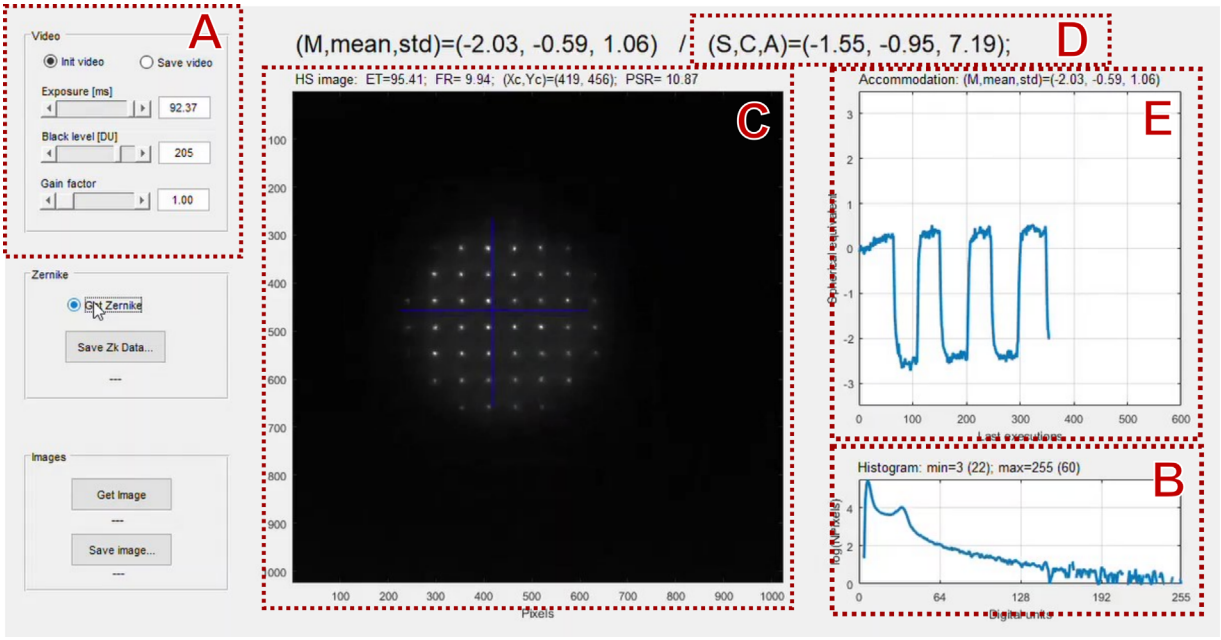

Figure 2. Image of the graphical user interface (GUI) with its main functional blocks labeled: video control (A), histogram (B), HS image (C), current refraction state (D), and variations in the spherical refractive state with time (E).

light from a laser diode (LD) emitting at 830 nm reaches the aperture (P1). This element limits the size of the beam entering the eye to a diameter of 1.5 mm. After P1, the light is transmitted through the linear polarizer (B1) and beam splitter (BS) and reflected by the hot mirror (HM) before reaching the trial lenses of the phoropter (0.25-diopter [D] step changes for sphere and cylinder), which is placed in front of the eye. The HM allows the system to use infrared light without interfering with the visual field of the patient. During measurements, the eye is exposed to 10 µW, which is well within the safety limits.[29] At the working wavelength and radiation power, the laser beacon is barely observable, but the low visibility[30] makes measurements more comfortable for patients. Based on the changes found in the pupil size in a young, healthy eye that are detected when turning the laser on and off, a negligible pupil constriction is expected due to the laser beacon emitted by the system.

After being backscattered by the ocular fundus, the light follows a path similar to that described above until it reaches the BS. This element redirects the light toward linear polarizer B2, which has a polarization axis perpendicular to that of linear polarizer B1 so that corneal reflections are considerably attenuated. In order to fully avoid the corneal reflections, the laser beam enters the eye slightly (1 mm) off-centered with respect to the corneal apex. Then, the light passes through lens L1, is reflected by the mirror (M), and passes through lens LF, bandpass filter F with peak transmission at the working wavelength, and lens L2 before reaching the HS sensor formed by lenslet array LHS followed by the complementary metal-oxide semiconductor (CMOS) sensor (CHS). Lenses L1 and L2, whose focal lengths are 50 and 30 mm, respectively, form a telescope that permits the pupil of the eye and lenslet array LHS at conjugate planes with a magnification of $m = -0.6$. The zero of the system was obtained using an artificial eye composed of an achromatic lens with cardboard acting as the retina positioned nominally at its focal plane. The inclusion of field lens LF with a focal length of −18 mm allows the instrument to be compact, despite the increase in the distance needed for coupling the system without interfering with the handling of the phoropter. Regarding the HS sensor, lenslet array LHS has a pitch and focal length of 300 µm and 5.1 mm, respectively, whereas CHS captures images of 1024 × 1024 pixels with a resolution of 5.3 µm.

The system described above was placed inside a box with internal dimensions of 120 × 120 × 120 mm^3 and mounted on a rail that allows the lateral shift to align the system with the subject's right and left eyes. The HS sensor is controlled remotely through a graphical user interface that permits setting the parameters of the camera and showing the current HS image and associated refractive state of the eye (Fig. 2). An HS image is processed every 100 ms; therefore, 10 estimations of the refractive state are available every second. The processed data were automatically saved in a text

file when the video was deactivated. In addition to information regarding wavefront aberrations, statistical data of the gray intensity levels in the HS image were recorded. Although wavefront aberrations are used to compute the refractive state following a paraxial curvature matching approximation using the second- and fourth-order Zernike coefficients,[31] statistical data are employed by the data processing algorithm to automatically detect blinks and misalignments between the optical axis of the eye and the system.

Unless stated otherwise, the estimations of the ocular refractive state presented in this study are given in power vector notation (M, J_0, J_{45}).[32,33] Although measurements were performed in an open field and for natural pupils, the Zernike coefficients were computed over a pupil 3.5 mm in diameter, which is a size that enables the estimation of low-order aberrations[34] and permits a maximum misalignment between the eye and the optical axis of the system of 2.75 mm without leaving the measurement region of the HS sensor.

Measurement of the Accommodation Response

The instrument described above was tested through an experimental study conducted at the Centre Universitari de la Visió of the Universitat Politècnica de Catalunya. This observational study was approved by the ethics committee of the Hospital Universitari Mútua Terrassa and conformed to the tenets of the Declaration of Helsinki. All participants signed a written informed consent after the purpose and procedure of the trial were explained to them. Inclusion criteria were age over 18 years, distance visual acuity measured with a Snellen chart of at least 0.8 (decimal notation), subjective spherical equivalent refraction between ±6 D, and maximum magnitude of astigmatism of 3 D, which are within the operating range of the system and suitable for most of the population.[35] Patients with ocular pathologies, binocular dysfunctions at a far distance, or any other condition that prevented standard subjective refraction were excluded.

In every session, the objective spherical equivalent refraction (M_O) was first measured using the open-field autorefractometer Grand Seiko WAM 5500 (Shigiya Machinery Works, Fukuyama, Japan).[22] Next, participants were placed and properly aligned with the instrument coupled to the phoropter described above. Eventual ametropia taken from the known manifest refraction (M_S, J_{0S}, J_{45S}), previously assessed by an optometrist, was properly translated into the phoropter, and it was considered as the reference refraction. Subsequently, real-time variations in the refractive state due to changes in the accommodation were estimated with the developed instrument while placing the reference refraction plus a set of trial lenses in the phoropter with the following spherical equivalent power differences (ΔM) in this order: +2, +1.50, +1, +0.75, +0.50, +0.25, 0, −0.25, −0.50, −1, −1.50, and −2 D. Each trial lens was kept in front of the eye for at least 10 seconds. Therefore, approximately 100 estimations of the refractive state were available for each trial lens. During measurements, the subject was asked to stare at a Snellen chart positioned 4 meters away from the phoropter while blinking normally. On average, the sweep of the trial lenses was completed in approximately 120 seconds. The process was performed for the right eye and then repeated for the left eye, with a resting time of 1 minute in between.

Data Processing

Real-time estimations of the refractive state were postprocessed as follows: First, the gray levels of the HS spots measured using the instrument were used to discard all estimations whose images showed a mean intensity below a given threshold. The purpose was to exclude data obtained during blinks from the analysis. Subsequently, the mean spherical equivalent (M_Δ) was obtained considering all the non-discarded estimations available for each trial lens after compensating for chromatic aberrations by adding −0.83 D to the estimated values as measurements were carried out in the infrared.[36]

The values of M_Δ as a function of the trial lens represent a curve that includes the contribution to the optics of the eye and the phoropter (reference refraction plus trial lens). Therefore, accommodation-related changes of the steady-state spherical equivalent response of the eye (MR) were obtained relative to the reference refraction after removing from M_Δ the contribution of the trial lenses placed in the phoropter using Equation 1:

$$MR = M_\Delta + \Delta M + 0.25D \quad (1)$$

where 0.25 stands for the expected spherical refractive error when looking at a target located at 4 meters. In this study, the AR is defined as the negative MR for the set of trial lenses placed in front of the eye with the phoropter. Using this definition, an increase in the optical power of the eye due to accommodation was registered as an increase in AR.

To estimate the spherical equivalent refraction of the eye from the measured data (M_E), we considered the MR value measured at $\Delta M = 0$ after removing the contribution of the reference refraction. For validation

purposes, the M_E estimations were compared with the objective values of M_O, which were obtained using the Grand Seiko WAM 5500.

Statistical Analysis

Statistical analysis was performed using SPSS Statistics 24 for Windows (IBM, Chicago, IL). In all cases, a 95% confidence interval was used; $P < 0.05$ was considered statistically significant. The Kolmogorov–Smirnov test was used to evaluate the normal distribution of all variables. The right or left eye of each subject was randomly selected for analysis to avoid any bias due to inter-eye correlation. Bivariate Pearson's correlation coefficient (r), related-sample t-test, and Bland–Altman analysis were used to study the agreement between M_S and M_O and between M_S and M_E. The 95% limits of agreement (LoA) were calculated as 1.96 times the standard deviation (SD) of the mean difference. A multivariate general linear model using the AR values for the different trial lenses as the dependent variables was used to assess the effect of age and M_S on AR, and the effect size (partial eta-squared η_p^2) was calculated (small = 0.01, medium = 0.06, and large = 0.14).[37]

Results

Seventy-three volunteers between 19 and 69 years of age were included in the study (50 women and 23 men; mean age ± SD, 29.8 ± 12.9 years). The analysis presented here corresponds to data from 37 and 36 randomly selected right and left eyes, respectively. The mean ± SD and ranges of the spherical equivalent refractions M_S, M_O, and M_E for the selected eyes are shown in Table 1.

The agreement between the spherical equivalent refractions M_S and M_O and between M_S and M_E can be observed in the Bland–Altman plots in Figure 3. With respect to M_S, the objective values M_O obtained with the commercial device presented a lower mean of the differences (mean = −0.14 D, $P = 0.212$ vs. −0.48 D, $P < 0.001$). However, the M_E estimations obtained with our system presented a lower range in terms of the 95% LoA (range, 1.24 vs. 1.87 D) and a better correlation

Table 1. M_S, M_O, and M_E for the 37 Right and 36 Left Eyes Randomly Selected

	Diopters		
Parameter	M_S	M_O	M_E
Mean ± SD	−1.22 ± 1.98	−1.08 ± 1.85	−0.49 ± 1.90
Range (min, max)	(−5.38, +5.00)	(−4.88, +3.75)	(−4.79, +5.42)

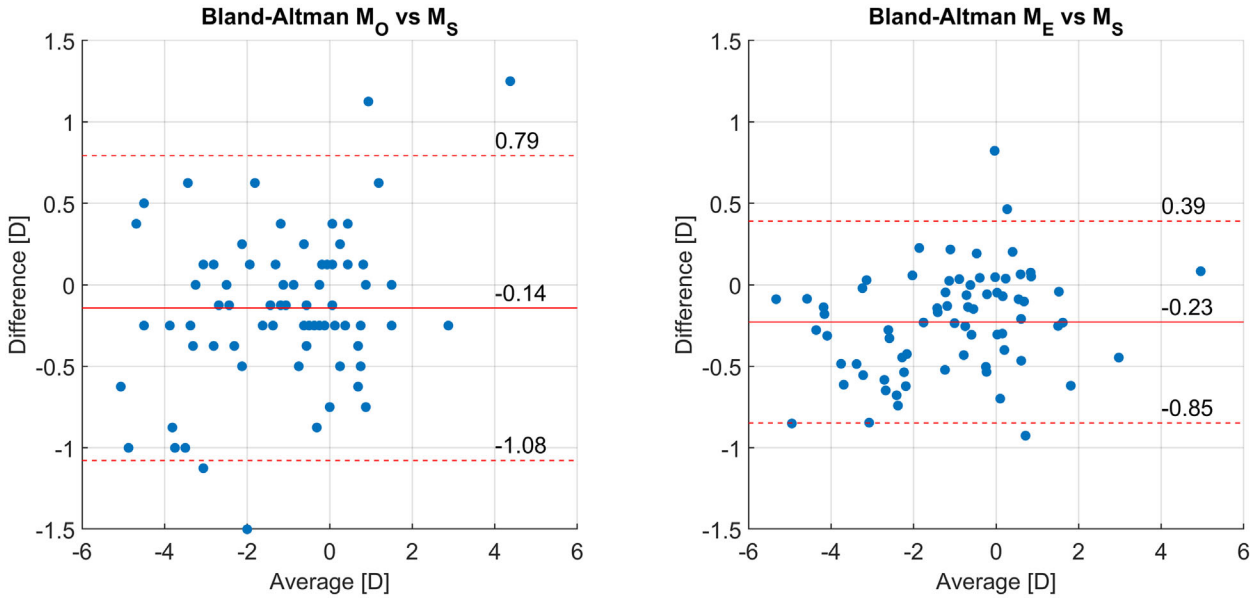

Figure 3. Bland–Altman plots showing agreement between M_O and M_S (*left*) and between M_E and M_S (right) for the 73 analyzed eyes. The mean of the differences (*continuous line*) and the 95% LoAs (*discontinuous lines*) are indicated in the plots.

Table 2. Within-Subjects Analysis of Variance *F*-test, *P*, and η_p^2 Values for Age and M_S

		ΔM (D)												
		+2.00	+1.50	+1.00	+0.75	+0.50	+0.25	0.00	−0.25	−0.50	−0.75	−1.00	−1.50	−2.00
Age	*F*	0.01	0.01	0.47	0.65	0.27	0.10	0.60	1.58	4.27	8.43	14.97	22.57	55.94
	P	0.931	0.912	0.494	0.421	0.600	0.742	0.439	0.212	**0.042**	**0.005**	**0.000**	**0.000**	**0.000**
	η_p^2	0.000	0.000	0.007	0.009	0.004	0.002	0.008	0.022	**0.057**	**0.106**	**0.174**	**0.241**	**0.441**
M_S	*F*	7.97	8.29	7.94	9.53	10.03	9.32	8.10	3.06	0.56	0.14	0.02	0.35	0.00
	P	**0.006**	**0.005**	**0.006**	**0.003**	**0.002**	**0.003**	**0.006**	0.085	0.456	0.707	0.875	0.552	0.971
	η_p^2	**0.101**	**0.105**	**0.101**	**0.118**	**0.124**	**0.116**	**0.103**	0.041	0.008	0.002	0.000	0.005	0.000

Statistically significant *P* values and medium and large effect sizes are indicated in bold.

Table 3. Spherical Equivalents for M_S, M_O, and M_E for the Four Subgroups

		Spherical Equivalents (D)			
			Young		
	Parameter	Adult ($n = 19$)	All ($n = 54$)	Myopic ($n = 36$)	Non-Myopic ($n = 18$)
M_S	Mean ± SD	−0.27 ± 1.59	−1.55 ± 2.01	−2.61 ± 1.39	0.56 ± 1.23
	Range (min, max)	(−4.25, 2.75)	(−5.38, 5.00)	(−5.38, 0.50)	(−0.38, 5.00)
M_O	Mean ± SD	−0.14 ± 1.54	−1.41 ± 1.85	−2.38 ± 1.35	0.54 ± 0.94
	Range (min, max)	(−3.25, 3.00)	(−4.88, 3.75)	(−4.88, −0.25)	(−0.25, 3.75)
M_E	Mean ± SD	0.63 ± 1.63	−0.55 ± 1.90	−1.54 ± 1.32	1.45 ± 1.18
	Range (min, max)	(−3.57, 3.70)	(−4.79, 5.42)	(−5.79, 0.53)	(−0.07, 5.42)

($r = 0.989$, $P < 0.001$ vs. $r = 0.955$, $P < 0.001$) with the subjective values.

Table 2 shows for each value ΔM of the trial lenses, the analysis of variance within subjects, introducing age and M_S as covariates into the AR model. As shown, the effect size of age was negligible in the fogging interval between +2.00 D and −0.25 D lens trial. However, it was medium for the −0.50 D trial and increased progressively up to the maximum stimulus of −2.00 D, in which the effect size was large. In contrast, M_S had a medium effect size throughout the fogging range but was negligible for the negative lens trial range.

The capacity of the system to determine changes in accommodation as a function of the trial lens, that is, the obtainment of the AR, was analyzed considering the influence of age and M_S in the measured responses described above. First, the sample was divided into the following age subgroups: young (age ≤ 30 years; mean ± SD = 23 ± 3 years) and adult (age > 30 years; mean ± SD = 49 ± 10 years). It should be noted that the ARs for these two subgroups are expected to differ due to the influence of age on accommodation.[38] In addition, the young subgroup was subdivided into myopic subjects ($M_S \leq -0.5$ D) and non-myopic subjects ($M_S > -0.5$ D) according to the subjective refraction.[39] The influence of age is expected to be negligible in the second subdivision. Statistical information about the spherical equivalents M_S, M_O, and M_E for the resulting subgroups are listed in Table 3.

Specific examples of the AR measured for volunteers 005 and 021, as well as the mean ARs as a function of the trial lens for the four subgroups are shown in Figure 4. In general, the response may be divided into two main regions: one between +2 D and 0 D (trial lenses with $\Delta M \geq 0$ D) and the other between 0 and −2 D (trial lenses with $\Delta M \leq 0$ D). In the first region, the trial lens with positive spherical power induces pseudo-myopia in the eye under analysis, thus relaxing accommodation, as in the fogging technique; consequently, the measured response remains constant. In contrast, in the second region, the accommodation is active, and its magnitude increases to compensate for the trial lens with $\Delta M < 0$ D placed in the phoropter.

In the specific examples, a visual inspection of the responses shows that transitions between relaxed and active accommodation occurred for trial lenses with ΔM of −0.50 D and +0.50 D for volunteers 005 (female, 25 years old; $M_S = -1$ D, $M_E = -0.07$ D) and 021 (female, 21 years old; $M_S = -1.50$ D, $M_E = -1.54$ D), respectively. At such values, the error bars,

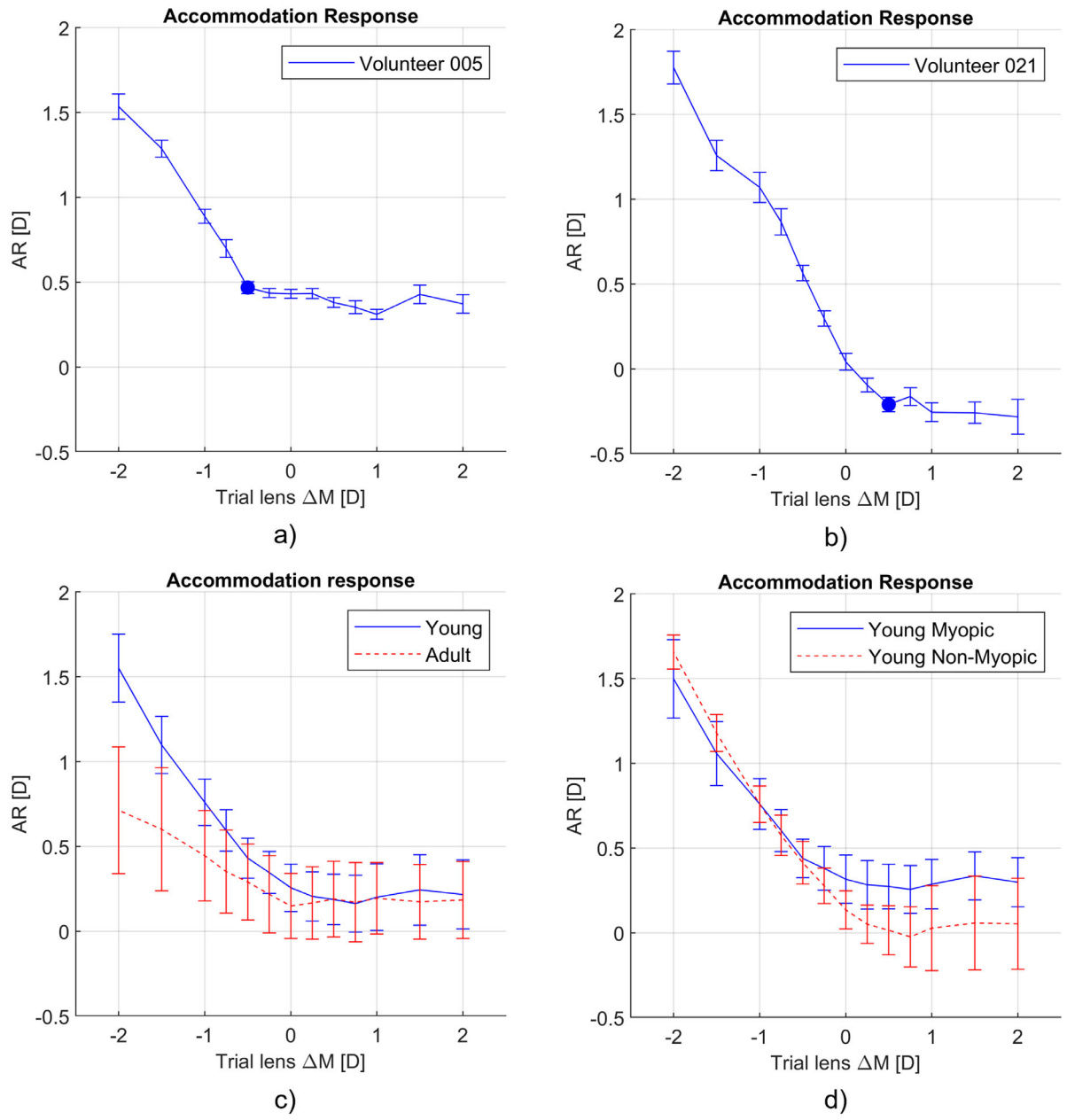

Figure 4. (*Top*) Individual ARs as a function of the ΔM trials for volunteers 005 (a) and 021 (b). (*Bottom*) Mean accommodative response as a function of ΔM for young (c, *continuous blue line*) and adult (c, *discontinuous red line*) subjects and for young myopic (d, *continuous blue line*) and young non-myopic (d, *discontinuous red line*) subjects The *error bars* represent 1 SD of the fluctuations in ARs (*top*) and the variability between subjects (*bottom*) for each trial lens. The *blue circles* indicate the transition between relaxed and active accommodation obtained by visual inspection (*top*).

which represent the AR fluctuations considering the 100 measurements available for each trial lens, also presented their minimum values. In the mean curves, the ARs presented differences among the measured groups, as expected from the analysis of variance summarized in Table 2. When analyzing the groups divided by age within the region in which the influence of this parameter caused statistical differences (trial lenses with ΔM between −0.5 D and −2 D), we found values of $m = 0.77$ and 0.29 for the slopes in the measured AR for young and adult subjects, respectively.

Regarding the groups of young subjects classified by ametropia, the AR presented a similar (stable) behavior but with a different magnitude along the region in which the influence of MS caused statistical

differences (trial lenses with ΔM between +2 D and 0 D). With the reference being the minimum value of AR, the responses decreased from +0.26 D for the myopic group to +0.02 D for the non-myopic one; in other words, a difference in magnitude of 0.28 D between these two groups was observed in the region where accommodation was relaxed. The error bars representing the SD of our population indicate that there is lower inter-subject variability in the myopic group when accommodation is not stimulated (trial lenses with ΔM > 0 D). For example, for the extreme value of +2 D, the myopic and non-myopic groups showed SDs of 0.29 D and 0.53 D, respectively. In contrast, this dispersion was higher in the myopic group as the accommodation demand increased (trial lenses with ΔM < 0 D). For −2 D, the myopic and non-myopic groups presented SDs of 0.46 D and 0.20 D, respectively.

Discussion

One of the goals of this study was to test the developed instrument as a means of measuring the refractive state of the eye every 100 ms, a sampling rate that allows the instrument to obtain representative estimates of the steady-state AR.[40–42] Although the instrument also provides information about astigmatism and HOAs, this study focuses on the analysis of accommodation-related changes in spherical refraction M, whose negative value is the parameter used to account for accommodation. Errors in focus followed by spherical aberrations are the main cause of image degradation in an accommodated eye,[9,10,31] which are actually included in the metric used for obtaining M (paraxial curvature matching) and may be well estimated using the fourth-order Zernike coefficients used in the developed instrument.[43,44] As shown in Figure 3, the estimations of the spherical equivalent (M_E) obtained with the system showed a good correlation (precision) with the subjective refraction values (M_S), as indicated by the 95% LoA between these two estimations. Such a correlation was close to that observed between the objective values (M_O) measured with the commercial autorefractor and the subjective refraction (M_S). Although the instrument used as a reference has been widely proven effective in measuring refractive errors,[22] the better correlation between our system and the subjective refraction may be attributed to the differences in the methodology followed. For the autorefractor, measurements were performed in open field and binocular vision, but no attention was given to the control of accommodation. In our measurements, the estimation corresponded to data obtained after the ΔM values of the trial lenses presented in front of the eye decreased gradually from +2 D to 0 D in the phoropter. The addition of trial lenses with ΔM > 0 should relax (deactivate) accommodation,[8,13] thus reducing errors due to stimulated accommodation in our measurements. Additionally, the estimations obtained are comparable to those of other systems reported in the literature.[23,26] For example, in Carracedo et al.,[23] a range of about 1.7 D (95% LoA) is given as the difference between the estimations of the spherical refractive error and the subjective refraction using a system that integrates a HS sensor to a system that fulfills the functionalities of a phoropter.

The mean differences in magnitude between the spherical equivalents M_E estimated with the system and the subjective values (accuracy) might be attributed to the fact that participants were positioned 4 meters from the visual target, and for that a general correction of 0.25 D was applied; however, the real accommodative lag or lead at this distance for each participant was unknown. Other systematic errors may have also contributed to the mean differences between M_E and M_S. The estimations of the system were corrected for chromatic aberrations during data processing. Therefore, the differences may have been due to a residual defocus in our reference image used to obtain the positions of the spots in the HS image for 0 D. In our system, such an image was obtained using an artificial eye composed of an achromatic lens with cardboard acting as the retina positioned nominally at its focal plane. Regardless of the cause, this offset should be incorporated into the software in the future after testing a larger number of eyes to avoid this interference in the computation of the refractive state.

The system coupled to a phoropter allowed us to obtain the AR of patients from real-time estimations of the refractive state of the eye while placing a set of trial lenses that added spherical power to the subjective refraction. In terms of shape, the behavior of the AR shown in Figure 4 was expected.[13] Such responses are composed of a region with a practically constant value and another with an increasing value as ΔM decreases after a transition point. In the latter case, the increment in magnitude is attributed to the fact that accommodation was active to compensate for the trial lens with ΔM < 0 D placed in the phoropter.

It has been proven that the AR is highly influenced by age, as shown by an effect size of up to 44% for the 2-D stimulus used during the measurements, as shown in Table 2. The loss of accommodation capacity with age is shown in Figure 4c. In the region where the response presented statistically

significant differences, the AR was linked to slopes within the range reported in Radhakrishnan and Charman,[14] who found variation in accommodation between 0.8 D and 0.7 D per diopter of stimulation for patients under 30 years. It has been reported elsewhere that, at this age, accommodation capacity starts to decline more rapidly.[38] Although this behavior of accommodation with age was already expected, the similarities between our results and those reported by other authors demonstrate the capacity of our system to provide true estimations of the AR of the eye.

It was found that M_S also had an influence on AR in the accommodation relaxation interval (trial lenses with $\Delta M > 0$ D), with an effect size of approximately 10%. In the young population grouped as myopic and non-myopic subjects, a comparison of the error bars in Figure 4d indicates that the responses of myopic eyes showed higher intersubject variability for trial lenses with $\Delta M < 0$ D, whereas in non-myopic subjects, maximum dispersion was found for trial lenses with $\Delta M > 0$ D. This behavior appears to agree with data for the two groups reported by other studies[13,19,45] and could be explained by the effects of unquantified HOAs (spherical aberrations) under the measurement conditions[19,20,46] and variations in the lag of accommodation with refractive error observed in myopes.[47]

The differences between the ARs of young myopic and non-myopic subjects can be seen in Figure 4d as the difference in the values registered for trial lenses with $\Delta M > 0$ D. In our measurements, such a higher value should not be interpreted as a stronger accommodation for the myopic group but rather as a higher offset in the measured response that might be caused by a disagreement between the refraction used as a reference (manifest subjective refraction) and the refraction of the eye due to optical factors. Because accommodation is computed as the negative of M, a lower value indicates that, for the reference refraction, non-myopic eyes presented residual refraction of about +0.36 D as compared to myopic eyes. However, this difference is well within the reliability of manifest subjective refraction, which has been reported elsewhere and is 0.25 D or 0.50 D.[48]

Information on the behavior of accommodation can be used by clinicians to validate the subjective procedure that they generally performed. For example, let us consider that the individual ARs shown in Figure 4 (top) for volunteers 005 and 021 correspond to the measurements during subjective refraction. At the end of the test, the optometrist would be capable of analyzing the objective ARs and making decisions about the refraction found. In particular, for volunteers 005 and 021, the results in terms of the transition point would suggest corrections of −0.5 D and +0.50 D, respectively, from the reference refraction found.

Wavefront sensing allows access to pupil size and spherical aberration data, information that permits a better understanding of the accommodation process.[43,49] A limitation of this study is that pupil size was not monitored and, consequently, the accommodation was available for a fixed pupil size. Using the rate of pupil constriction per diopter of accommodation (miosis) of 0.18 mm/D reported elsewhere,[9] we would expect variations in the pupil size of about 0.36 mm in the stimulated range. Regarding the use of a fixed pupil, simulations of the effects on accommodation of spherical aberrations predict a difference of 0.16 D in the range from 0 to 2 D between the accommodative responses computed for a fixed 4-mm pupil diameter and the one obtained when the effects of miosis are considered.[43] Therefore, taking into account that illumination conditions were the same for all participants during measurements and that there was a limited accommodative demand (and consequent miosis), few variations were expected in the pupil size and in the accommodation-related changes of HOA. However, these assumptions should be corroborated in future work.

In summary, the developed instrument can be used as a supporting tool during any clinical procedure in which accommodation plays a role. The instrument showed good precision in estimating the refractive state of the eye and was able to obtain an AR when working in combination with a phoropter. Additionally, the instrument may also be used to provide information about the instantaneous refractive state without interfering with subjective refraction. After this process, clinicians would have information about the accommodative response during the test, helping them to validate the results and make any additional decisions if necessary. Finally, the results presented here could be used in the future to study the effects of the fogging technique during subjective refraction or to develop new methodologies for objective refractive error estimations based on analysis of the AR.

Acknowledgments

This publication is part of the project PID2020-112527RB-I00, funded by MCIN/AEI/10.13039/501100011033, and the Miopmilla Program, funded by the Official College of Opticians and Optometrists of Catalonia. Aina Turull-Mallofré gratefully acknowledges the Universitat Politècnica de Catalunya and Banco Santander for the financial support of her

predoctoral grant FPI-UPC. Mikel Aldaba is a Serra Húnter Fellow.

Disclosure: **C.E. García-Guerra**, None; **J.A. Martínez-Roda**, None; **J.C. Ondategui-Parra**, None; **A. Turull-Mallofré**, None; **M. Aldaba**, None; **M. Vilaseca**, None

References

1. Rabbetts RB. *Clinical Visual Optics*. Oxford, UK: Butterworth-Heinemann Limited; 1997.
2. Borish IM. *Borish's Clinical Refraction*. Philadelphia, PA: W.B. Saunders Company; 1998.
3. Maul E, Borroso S, Munoz SR, Sperduto RD, Ellwein LB. Refractive error study in children: results from La Florida, Chile. *Am J Ophthalmol*. 2000;129(4):445–454.
4. Fotedar R, Rochtchina E, Morgan I, Wang JJ, Mitchell P, Rose KA. Necessity of cycloplegia for assessing refractive error in 12-year-old children: a population-based study. *Am J Ophthalmol*. 2007;144(2):307–309.
5. Morgan IG, Iribarren R, Fotouhi A, Grzybowski A. Cycloplegic refraction is the gold standard for epidemiological studies. *Acta Ophthalmol (Copenh)*. 2015;93(6):581–585.
6. Hopkins S, Sampson GP, Hendicott P, Lacherez P, Wood JM. Refraction in children: a comparison of two methods of accommodation control. *Optom Vis Sci*. 2012;89(12):1734–1739.
7. Reese EE, Fry GA. The effect of fogging lenses on accommodation. *Optom Vis Sci*. 1941;18(1):9–16.
8. Queirós A, González-Méijome J, Jorge J. Influence of fogging lenses and cycloplegia on open-field automatic refraction. *Ophthalmic Physiol Opt*. 2008;28(4):387–392.
9. Plainis S, Ginis HS, Pallikaris A. The effect of ocular aberrations on steady-state errors of accommodative response. *J Vis*. 2005;5(5):466–477.
10. Charman WN. The eye in focus: accommodation and presbyopia. *Clin Exp Optom*. 2008;91(3):207–225.
11. Radhakrishnan H, Allen PM, Charman WN. Dynamics of accommodative facility in myopes. *Invest Ophthalmol Vis Sci*. 2007;48(9):4375–4382.
12. McBrien NA, Millodot M. The relationship between tonic accommodation and refractive error. *Invest Ophthalmol Vis Sci*. 1987;28(6):997–1004.
13. Ward PA, Charman WN. An objective assessment of the effect of fogging on accommodation. *Am J Optom Physiol Opt*. 1987;64(10):762–767.
14. Radhakrishnan H, Charman WN. Age-related changes in static accommodation and accommodative miosis. *Ophthalmic Physiol Opt*. 2007;27(4):342–352.
15. Chirre E, Prieto P, Artal P. Dynamics of the near response under natural viewing conditions with an open-view sensor. *Biomed Opt Express*. 2015;6(10):4200–4211.
16. Liang J, Grimm B, Goelz S, Bille JF. Objective measurement of wave aberrations of the human eye with the use of a Hartmann-Shack wavefront sensor. *J Opt Soc Am A Opt Image Sci Vis*. 1994;11(7):1949–1957.
17. Tarrant J, Roorda A, Wildsoet CF. Determining the accommodative response from wavefront aberrations. *J Vis*. 2010;10(5):4.
18. Gambra E, Sawides L, Dorronsoro C, Marcos S. Accommodative lag and fluctuations when optical aberrations are manipulated. *J Vis*. 2009;9(6):4.1–15.
19. He JC, Gwiazda J, Thorn F, Held R, Vera-Diaz FA. The association of wavefront aberration and accommodative lag in myopes. *Vision Res*. 2005;45(3):285–290.
20. Paquin MP, Hamam H, Simonet P. Objective measurement of optical aberrations in myopic eyes. *Optom Vis Sci*. 2002;79(5):285–291.
21. Vedhakrishnan S, de Castro A, Vinas M, Aissati S, Marcos S. Accommodation through simulated multifocal optics. *Biomed Opt Express*. 2022;13(12):6695–6710.
22. Sheppard AL, Davies LN. Clinical evaluation of the Grand Seiko Auto Ref/Keratometer WAM-5500. *Ophthalmic Physiol Opt*. 2010;30(2):143–151.
23. Carracedo G, Carpena-Torres C, Serramito M, Batres-Valderas L, Gonzalez-Bergaz A. Comparison between aberrometry-based binocular refraction and subjective refraction. *Transl Vis Sci Technol*. 2018;7(4):11.
24. Cheng X, Himebaugh NL, Kollbaum PS, Thibos LN, Bradley A. Validation of a clinical Shack-Hartmann aberrometer. *Optom Vis Sci*. 2003;80(8):587–595.
25. Agarwal A, Bloom DE, deLuise VP, Lubet A, Murali K, Sastry SM. Comparing low-cost handheld autorefractors: a practical approach to measuring refraction in low-resource settings. *PLoS One*. 2019;14(10):e0219501.
26. Durr NJ, Dave SR, Vera-Diaz FA, et al. Design and clinical evaluation of a handheld wavefront autorefractor. *Optom Vis Sci*. 2015;92(12):1140–1147.
27. Jorge J, Queirós A, Almeida JB, Parafita MA. Retinoscopy/autorefraction: which is the best

starting point for a noncycloplegic refraction? *Optom Vis Sci*. 2005;82(1):64–68.
28. Jorge J, Queirós A, Gonzalez-Meijome J, Fernandes P, Almeida JB, Parafita MA. The influence of cycloplegia in objective refraction. *Ophthalmic Physiol Opt*. 2005;25(4):340–345.
29. UNE. *UNE-EN 60825-1: Seguridad de los productos láser. Parte 1: Clasificación de los equipos y requisitos.* Madrid, Spain: Asociación Española de Normalización y Certificación; 2014.
30. Sliney DH, Wangemann RT, Franks JK, Wolbarsht ML. Visual sensitivity of the eye to infrared laser radiation. *J Opt Soc Am*. 1976;66(4):339–341.
31. Thibos LN, Xin H, Bradley A, Applegate RA. Accuracy and precision of objective refraction from wavefront aberrations. *J Vis*. 2004;4(4):329–351.
32. Thibos LN, Wheeler W, Horner D. Power vectors: an application of Fourier analysis to the description and statistical analysis of refractive error. *Optom Vis Sci*. 1997;74(6):367–375.
33. Thibos LN, Horner D. Power vector analysis of the optical outcome of refractive surgery. *J Cataract Refract Surg*. 2001;27(1):80–85.
34. Liang J, Williams DR. Aberrations and retinal image quality of the normal human eye. *J Opt Soc Am A*. 1997;14(11):2873–2883.
35. Williams KM, Verhoeven VJ, Cumberland P, et al. Prevalence of refractive error in Europe: the European Eye Epidemiology (E^3) Consortium. *Eur J Epidemiol*. 2015;30(4):305–315.
36. Thibos LN, Ye M, Zhang X, Bradley A. The chromatic eye: a new reduced-eye model of ocular chromatic aberration in humans. *Appl Opt*. 1992;31(19):3594–3600.
37. Cohen J. *Statistical Power Analysis for the Behavioral Sciences*. 2nd ed. Mahwah, NJ: Lawrence Erlbaum Associates; 1988.
38. Kalsi M, Heron G, Charman WN. Changes in the static accommodation response with age. *Ophthalmic Physiol Opt*. 2001;21(1):77–84.
39. Flitcroft DI, He M, Jonas JB, et al. IMI – Defining and classifying myopia: a proposed set of standards for clinical and epidemiologic studies. *Invest Ophthalmol Vis Sci*. 2019;60(3):M20–M30.
40. Labhishetty V, Bobier WR, Lakshminarayanan V. Is 25Hz enough to accurately measure a dynamic change in the ocular accommodation? *J Optom*. 2019;12(1):22–29.
41. Charman WN, Heron G. Fluctuations in accommodation: a review. *Ophthalmic Physiol Opt*. 1988;8(2):153–164.
42. Charman WN, Heron G. Microfluctuations in accommodation: an update on their characteristics and possible role. *Ophthalmic Physiol Opt*. 2015;35(5):476–499.
43. López-Gil N, Fernández-Sánchez V. The change of spherical aberration during accommodation and its effect on the accommodation response. *J Vis*. 2010;10(13):1–15.
44. Cheng H, Barnett JK, Vilupuru AS, et al. A population study on changes in wave aberrations with accommodation. *J Vis*. 2004;4(4):272–280.
45. Taylor J, Charman WN, O'Donnell C, Radhakrishnan H. Effect of target spatial frequency on accommodative response in myopes and emmetropes. *J Vis*. 2009;9(1):16.
46. Kaphle D, Varnas SR, Schmid KL, Suheimat M, Leube A, Atchison DA. Accommodation lags are higher in myopia than in emmetropia: measurement methods and metrics matter. *Ophthalmic Physiol Opt*. 2022;42(5):1103–1114.
47. Ghoushchi VP, Mompeán J, Prieto PM, Artal P. Binocular dynamics of accommodation, convergence, and pupil size in myopes. *Biomed Opt Express*. 2021;12(6):3282–3295.
48. Goss D, Grosvenor T. Reliability of refraction–a literature review. *J Am Optom Assoc*. 1996;67(10):619–630.
49. Lara F, Bernal-Molina P, Fernández-Sánchez V, López-Gil N. Changes in the objective amplitude of accommodation with pupil size. *Optom Vis Sci*. 2014;91(10):1215–1220.